Chemosphere 338 (2023) 139552

Contents lists available at ScienceDirect

Chemosphere

journal homepage: www.elsevier.com/locate/chemosphere

Fingerprinting of chlorinated paraffins and their transformation products in plastic consumer products

O. Mendo Diaz [a,b,*], A. Tell [a,c], M. Knobloch [a,b], E. Canonica [a,c], C. Walder [a], A.M. Buser [d], U. Stalder [b], L. Bigler [b], S. Kern [c], D. Bleiner [a,b], N.V. Heeb [a]

[a] Swiss Federal Laboratories for Materials Science and Technology Empa, Überlandstrasse 129, 8600 Dübendorf, Switzerland
[b] Department of Chemistry, University of Zürich, Winterthurerstrasse 190, 8057, Zürich, Switzerland
[c] Zürich University of Applied Sciences ZHAW, Einsiedlerstrasse 31, 8820, Wädenswil, Switzerland
[d] Swiss Federal Office for the Environment, Monbijoustrasse 40, 3003, Bern, Switzerland

HIGHLIGHTS

- More than 16000 ions from high-resolution mass spectra were processed with RASER.
- About 140 CP-, 75 CO-, 50 CdiO- and 24 CtriO-homologues were assigned.
- Five parameters were deduced and used for fingerprinting of plastic items.
- Fingerprints of CPs from GC-ECNI- and LC-APCI-MS data were compared.

GRAPHICAL ABSTRACT

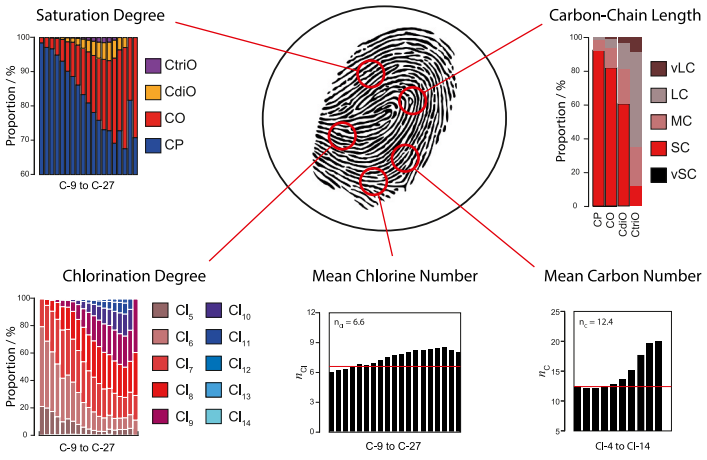

ARTICLE INFO

Handling Editor: J. de Boer

Keywords:
Persistent organic pollutants (POPs)
Short-chained chlorinated paraffins (SCCPs)
Homologue pattern
Fingerprinting of plastic materials
R-based automatic spectra evaluation routine (RASER)

ABSTRACT

Chlorinated paraffins (CPs) can be classified according to their length as short-chain (SC, C_{10}–C_{13}), medium-chain (MC, C_{14}–C_{17}) and long-chain (LC, $C_{\geq 18}$) CPs. Technical CP-mixtures can contain a wide range of carbon- (C-, n_C = 10–30) and chlorine- (Cl-, n_{Cl} = 3–19) homologues. CPs are high-production volume chemicals (>10^6 t/y). They are used as flame-retardants, plasticizers and coolant fluids. Due to the persistence, bioaccumulation, long-range environmental transport potential and adverse effects, SCCPs are regulated as persistent organic pollutants (POPs) by the Stockholm Convention. Transformation of CPs can lead to the formation of unsaturated compounds such as chlorinated mono- (CO), di- (CdiO) and tri-olefins (CtriO). Such transformation reactions can occur at different stages of CP manipulation providing characteristic C-/Cl-homologue distributions. All this results in unique patterns that collectively create a fingerprint, which can be distinguished from CP-containing samples. Therefore, CP-fingerprinting can develop into a promising tool for

* Corresponding author. Überlandstrasse 129, 8600 Dübendorf, Switzerland.
E-mail address: Oscar.mendodiaz@empa.ch (O. Mendo Diaz).

https://doi.org/10.1016/j.chemosphere.2023.139552
Received 18 January 2023; Received in revised form 14 July 2023; Accepted 16 July 2023
Available online 20 July 2023

future source apportionment studies and with it, the reduction of environmental burden of CPs and hazards to humans. Herein, CP-containing plastics were studied to establish fingerprints and develop this method. We analyzed four household items by reverse-phase liquid-chromatography coupled with a mass spectrometer with an atmospheric pressure chemical ionization source and an Orbitrap mass analyzer (RP-LC-APCI-Orbitrap-MS) operated at a resolution of 120000 (FWHM at *m/z* 200). MS-data of different CP-, CO-, CdiO- and CtriO-homologues were efficiently processed with an R-based automatic mass spectra evaluation routine (RASER). From the 16720 ions searched for, up to 4300 ions per sample were assigned to 340 C-/Cl-homologues of CPs and their transformation products. Specific fingerprints were deduced from the C-/Cl-homologues distributions, the carbon- (n_C) and chlorine- (n_{Cl}) numbers and saturation degree. These fingerprints were compared with the ones obtained by a GC-ECNI-Orbitrap-MS method.

1. Introduction

Chlorinated paraffins (CPs) are high-production volume chemicals (>1 million t/y) commonly used as flame retardants, plasticizers and coolant fluids (Barber et al., 2005; Glüge et al., 2016). Their chemical formula is $C_xH_{2x+2-y}Cl_y$ and depending on the number of carbons, CPs can be classified as short-chain (SC, C_{10}–C_{13}), medium-chain (MC, C_{14}–C_{17}) and long-chain (LC, $C_{\geq 18}$) CPs. Chlorine contents of technical CP mixtures vary from 30 to 70% by weight (De Boer, 2010). In this work, and following the nomenclature of a recent publication, C_9-, C_{18}–C_{21}- and $C_{\geq 22}$-CPs are further divided and named as very short-chain (vSC), long-chain (LC) and very long-chain (vLC) CPs, respectively (Knobloch et al., 2022a). In addition, molecules which differ in their carbon- (C_x, n_C) or chlorine- (Cl_y, n_{Cl}) numbers are defined here as carbon- (C-) or chlorine- (Cl-) homologues, respectively. Therefore, two series of homologues can be distinguished, one with variable *x* and constant *y* (C-homologues), and the other one with constant *x* and variable *y* (Cl-homologues).

SCCPs and MCCPs have been targeted by international regulatory affairs in the last two decades, whereas LCCPs remain uncontrolled. Due to their persistence, bioaccumulation, long-range environmental transport and adverse effects, SCCPs with a chlorine content greater than 48% by weight were listed in the Annex A of the Stockholm Convention with several specific exemptions (UNEP, 2017). As a result of their extensive production, use and inevitable release into the environment, CPs became ubiquitous worldwide (Vorkamp et al., 2019). Since 2021, MCCPs are classified as substances of concern too and are under revision (UNEP, 2021). Recent studies showed the presence of CPs in European markets emphasizing the proximity of humans to CPs either by skin contact or by dietary exposure (Carney Almroth and Slunge, 2022; Krätschmer et al., 2021). However, the exposure to CP transformation products such as chlorinated mono- (COs), di- (CdiOs) and tri- (CtriOs) olefins is less studied. These compounds can form from CPs after HCl-loss under enzymatic or thermal exposure (Heeb et al., 2019; Perkons et al., 2019; Schinkel et al., 2017), during metalwork (Schinkel et al., 2018c) or induced by the ionization source in mass spectrometry (Yuan et al., 2016). The detection of CPs and COs was in the spotlight, whereas the CdiOs and CtriOs were overlooked. Recently, CPs and olefinic material were found in plastic and environmental samples (Knobloch et al., 2022a; Wu et al., 2019). However, no method is established yet to evaluate efficiently C- and Cl-homologues of CPs and their transformation products.

Chemical fingerprinting has been introduced as a new method in the analysis of per- and polyfluoroalkyl substances (PFASs), which we believe is as useful for CPs and their transformation products (Charbonnet et al., 2021). Herein, pattern recognition by means of chemical composition is used to identify characteristic distributions of individual homologues resulting in specific fingerprints. Fingerprint of CPs were reported before but unsaturated material was not considered (Yuan et al., 2019). We think that complex homologue distributions of CPs and olefinic material provide interesting features to characterize them. The multidimensional analysis of CP pattern, including transformation products, in residual waters, wastewater treatment plants, waste materials in landfills and plastic consumer products in the markets can demonstrate the potential of fingerprinting (Brandsma et al., 2017; Li et al., 2021; McGrath et al., 2021; Zeng et al., 2012).

CP mixtures are intricate and pose an analytical challenge due to the presence of hundreds of C- and Cl-homologues, millions of isomers and the lack of well-characterized standard materials (De Boer, 2010; Fernandes et al., 2022; Schinkel et al., 2018a). Gas- (GC) and liquid- (LC) chromatography are used to fractionate CPs, although only a partial separation of homologues has been accomplished (Mézière et al., 2020; Tomasko et al., 2021; Wu et al., 2022). In combination with a mass spectrometer, CPs can be identified by their mass over charge ratio (*m/z*). However, mass interferences are abundant between different CPs and COs. Thus, a mass analyzer with a resolving power higher than 20000 is needed to resolve CP signals from the ones of their transformation products (Schinkel et al., 2018b). An LC-MS system equipped with an atmospheric pressure-chemical ionization (APCI) source and an Orbitrap mass analyzer proved to be successful in the analysis from SC- to LCCPs (Yuan et al., 2018). To our understanding, at least 374 CP homologues (C_9–C_{30}, Cl_3–Cl_{19}) should be considered in the analysis of CPs. Each C- and Cl-homologue provides a characteristic isotopic cluster in a mass spectrum based on the abundances of ^{12}C-, ^{13}C-, ^{35}Cl- and ^{37}Cl-isotopes. This results in mass spectra containing more than 16000 ions, which is tedious to evaluate when screening a large number of samples.

Household items from the Swedish market containing CPs were previously analyzed by GC-ECNI- and LC-APCI-Orbitrap-MS (Knobloch et al., 2022a; Schinkel et al., 2018a). We hypothesized that fingerprints of CPs and their transformation products can be extracted from C- and Cl-homologue distributions and the outcome depends on the chosen analytical method. Our approach to deduce characteristic fingerprints of plastic materials must include an assessment of the parameters such as the chlorination and saturation degree. In addition, the evaluation of carbon-chain length groups per saturation degree must be added due to legislation relevance. We applied an RP-LC-APCI-Orbitrap-MS method at resolution of 120000 (FWHM at *m/z* 200) that can detect these features and studied the fingerprints of four plastic items. Under the given APCI-conditions, $[M+Cl]^-$ adduct ions are favored (Yuan et al., 2018; Zencak and Oehme, 2004). The processing of the complex mass spectra, which might include up to 16000 ions, was facilitated by the efficient and selective R-based automatic spectra evaluation routine (RASER) (Knobloch et al., 2022a). Data evaluation resulted in five characteristic properties of the samples, which can be considered as a unique fingerprint. In addition, fingerprints obtained by GC-ECNI- and LC-APCI-Orbitrap-MS were compared. Such features can now be used to distinguish between plastic materials. The establishment of a CP fingerprint library can be employed in forensic fingerprint analysis to track hot spots, polluting sources, reduce environmental burdens and human exposure.

2. Materials and methods

2.1. Samples and chemicals

Four residual plastic samples from the Swedish market P1–P4 were provided by the Swedish Chemical Agency (KEMI, Sundbyberg, Sweden)

during 2017. A garden cloche (P1), yoga mat (P2), jump toy (P3) and the rain cover of a stroller (P4) were studied (Table S1). A blank containing solvent and internal standard (IS) was prepared. In addition, a plastic coating of an electronic cable provided by Swiss Federal Office for the Environment (FOEN, Bern, Switzerland) was used as control sample. The solvents dichloromethane (DCM), *n*-hexane, methanol (MeOH) and acetone were obtained from Biosolve (Valkenswaard, Netherlands). The IS used was an isotopically labelled 1,5,5,6,6,10-hexachlorodecane ($^{13}C_{10}H_{16}Cl_6$, Cambridge Isotope Laboratories, Tewksbury, MA, USA).

2.2. Sample preparation

Four residual plastic materials and the control sample were cut into small pieces, from which 0.5 g were further treated. Soxhlet extractions of the plastics and blank were carried out with DCM (60 mL, 40 °C, 4 h) and extracts were concentrated by evaporation to 20 mL. One aliquot of 2 mL per residual plastic sample were extracted, whereas three aliquots of 2 mL of the control sample were arranged. Dissolved plastic material was precipitated by adding 2 mL MeOH. Aliquots of these solutions were spiked with IS (20 ng) and loaded onto a normal-phase chromatographic column (0.8 g SiO_2, diameter 5 mm). The column was pre-cleaned with DCM (3 mL) and pre-conditioned with *n*-hexane (3 mL). Fractions 1 and 2 were collected with *n*-hexane (5 mL) and *n*-hexane/DCM (5 mL, 8:2), respectively. Fraction 2 was dried with N_2 stream at 30 °C. The residue was dissolved in MeOH (100 μL) and analyzed by RP-LC-APCI-Orbitrap-MS.

2.3. Mass spectrometric analysis

The CP-containing fractions 2 were analyzed using a liquid chromatographic system Dionex Ultimate 3000 system (Thermo Fisher Scientific, Waltham, MS, USA) with a C_{18}-reversed-phase column Zorbax SB C18 RRHD 1.8 μm, 3 mm × 50 mm (Agilent Technologies Santa Clara, CA, USA). Injection volume was 6 μL. The eluents were water (A) and a mixture of MeOH and DCM (9:1, B) with a flow rate of 0.4 mL min^{-1}. A solvent gradient starting from 60% A was held for 1 min, followed by a linear increase to 98% B during 15 min, which was maintained for 7 min. A linear decrease to 60% A within 1 min was applied and held for 1 min, resulting in the initial conditions. Chloride-adduct ions $[M+Cl]^-$ were formed by an APCI-source Ion MAX API (Thermo Fisher Scientific, Waltham, MS, USA) and detected by a Q Exactive Orbitrap mass analyzer (Thermo Fisher Scientific, Waltham, MS, USA). The Orbitrap was operated in full scan from *m/z* 80 to 1200 at 12 Hz scanning frequency with a resolution of 120000 (FWHM at *m/z* 200).

2.4. Mass spectra processing with RASER

A detailed procedure for the analysis of mass spectra with RASER is described elsewhere and herein briefly explained (Knobloch et al., 2022a). The workflow of RASER is displayed in Figure S1. Full-scan mass spectra were obtained in the retention time window from 7 to 21 min. The *m/z* range from 265 (C_9Cl_3) to 1102 ($C_{30}Cl_{19}$) was considered. Two background subtractions from 5 to 6 and 22 to 23 min were applied with the *FreeStyle* software (V1.8.51.0, Thermo Fisher Scientific, Waltham, MS, USA). Measured MS data were exported into a csv file and processed with RASER. The isotopic clusters of chloride-adduct ions $[M+Cl]^-$ of the CP-, CO-, CdiO- and CtriO-homologues were scrutinized. Isotopic patterns were simulated using the *EnviPat* package (V2.4, Eawag, Dübendorf, Switzerland) (Loos et al., 2015). Experimental signals were searched in the range of *m/z* ± 0.002 of the simulated ones and compared. The peak height of the detected isotopologues ($MS_{cts,\ Isotopologue(x)}$, counts) were corrected to the corresponding relative abundances of each isotopologue, giving the $I_{100\%,Isotopologue(x)}$ (counts) parameter, which is employed in method validation and further calculations (Equation (1)).

$$I_{100\%,Isotopologue\ (x)} = \frac{MS_{cts,Isotopologue\ (x)}}{Relative\ abundance_{Isotopologue\ (x)}} \quad \text{Eq. 1}$$

The $I_{100\%}$-values of the three most abundant isotopologues of an isotopic cluster were averaged providing the mean $I_{100\%}$ ($MI_{100\%}$, in counts). The script also provides a reconstructed isotopic cluster based on the experimental *m/z* data. For the four plastic samples, C-homologues between $C_{9–30}$ and Cl-homologues between $Cl_{3–19}$ were considered, which accounts for 374 C-/Cl-homologues (Table S1). Accordingly, also C-/Cl-homologues of COs ($C_{9–30}$ and $Cl_{3–17}$, 330 C-/Cl-homologues), CdiOs ($C_{9–30}$ and $Cl_{3–15}$, 286 C-/Cl-homologues) and CtriOs ($C_{9–30}$ and $Cl_{3–13}$, 242 C-/Cl-homologues) were searched for. Thus overall, mass spectra were analyzed for the occurrence of 16720 ions corresponding to a total of 1232 C-/Cl-homologues. After RASER was applied, manual validation was performed. The reconstructed and theoretical isotopic clusters of each homologue were visually compared. A C-/Cl-homologue was present when the $MI_{100\%}$ was above the threshold of 100 cts and the relative signals of the isotopologues from the reconstructed isotopic cluster did not differ more than 10% from the relative signals of the theoretical isotopic cluster. Interferences affecting one or multiple isotopologues may occur, which are exemplified as deformed isotopic clusters. In that case, the $MI_{100\%}$ was calculated with non-interfered signals.

2.5. Quality assurance

All material employed was washed with *n*-hexane and DCM to reduce CP contaminations. To assess it, the blank was prepared by following the same procedure as the plastic samples. In addition, samples were exposed to heat during the soxhlet extraction (40 °C). However, this procedure did not reach 150 °C, the temperature at which CPs transform into olefinic material (Schinkel et al., 2018c). The three aliquots of the control sample were measured twice (total of six times) to assess the variability of the LC-MS system. CPs, COs, CdiOs and CtriOs of sample P2, which was analyzed and reported in a previous publication, were evaluated again with RASER (Knobloch et al., 2022a). Respective data are discussed in the results section together with the four plastic samples and are shown in the supporting information. Finally, MS-signals corresponding to the olefinic material of the IS, a $^{13}C_{10}H_{16}Cl_6$-CP were not found.

3. Results and discussion

3.1. Selective and efficient analysis of mass spectra by RASER

CPs were detected in the blank from C_{14} to C_{16}-homologues with chlorination degrees between Cl_5 and Cl_7 with $MI_{100\%}$ of about 120–870 cts (Table S2). Olefinic material such as COs, CdiOs and CtriOs was not detected. The contribution of all CP-homologues (sum of $MI_{100\%}$) was 3283 cts, which corresponds to less than 0.05% of the sum of $MI_{100\%}$ in the plastic samples. Therefore, such contaminations were considered irrelevant. CPs in the range of C_{14}–C_{18} and Cl_4–Cl_{10} were detected in all injections of the control sample with an averaged standard deviation of 7.9%. COs and CdiOs were found too and the total $MI_{100\%}$ were 6.5% and 0.1% of the $MI_{100\%}$ of the CPs. The averaged standard deviations of COs and CdiOs were 9.4% and 11.3%, respectively (Table S3). Therefore, the variability associated to the laboratory work and instrumental analysis was approximately 10%. Full-scan and reconstructed (RMS) mass spectra of CPs, COs, CdiOs and CtriOs of plastic consumer products P1–P4 were obtained after processing high resolution LC-APCI-Orbitrap-MS data with RASER (Fig. 1 and S2). A total of 4311 and 4312 ions were assigned in P1 and P4 samples, respectively. Most ions were identified as CPs (~50%), whereas minor contributors were COs (~25%), CdiOs (~17%) and CtriOs (~8%). Respective data are listed in Table S1. Ions were detected in the *m/z* range from 278 until 839. As Figure S3

displays, mass interferences are abundant if not enough mass spectral resolution is achieved (Knobloch et al., 2022a). Chloroolefin signals were 11- to 13-fold lower than the ones of CPs. Respective chlorodiolefin and chlorotriolefin signals were 75- to 105-fold and 490- to 2740-fold less abundant than the ones of CPs, respectively. Signals corresponding to isotopic clusters of CP-, CO- and CtriO-homologues could be distinguished, whereas some signals of CdiO-homologues were interfered. Therefore, $MI_{100\%}$-values of the latter were calculated based on three non-interfered isotopologue signals. The RMS of sample P2 reported by Knobloch et al. contained 600 ions more than what we report (Knobloch et al., 2022a). This could be due to the instrumental variability on the less abundant homologues.

3.2. Mapping C- and Cl-homologues in plastic materials

The C-/Cl-homologue distributions of CPs (A), COs (B), CdiOs (C) and CtriOs (D) in plastic consumer products P1–P4 were obtained based on the relative $MI_{100\%}$ after the analysis by LC-APCI-MS (Fig. 2 and Tables S4–S7). These distributions are given as 3D-plots. In all plastic materials CPs, COs, CdiOs and CtriOs were found in a wide range of C- ($C_{9–27}$) and Cl- ($Cl_{4–16}$) homologues. Due to very low abundances of Cl_{15}- and Cl_{16}-homologues, data presented below correspond only to Cl_4-to Cl_{14}-homologues. Unimodal distributions were observed among these samples with distinct maxima for both, C- and Cl-homologues of CPs. Most abundant CP-homologues (MAH) were Cl_7-homologues in all samples with some variations for C-homologues (C_{12}–C_{14}). SCCPs were the major contributors in P1 (59.8%), P3 (88.2%) and P4 (92.2%), whereas MCCPs were dominant in P2 (74.8%). Traces of LC- and vLCCPs and higher chlorination degrees ($Cl_{>11}$) were found. Between 0.1 and 2.4% of the total CP signal can be assigned as LCCPs. The C-and Cl-homologue distributions of CPs and MAH of the plastic P2 agree with previous findings except for less abundant homologues (Knobloch et al., 2022a). In accordance with what was visually perceived in Fig. 1, long-chain material increased its relative abundance in olefinic material. For example in the P4 material, 1.4% long-chain chlorinated paraffins (LCCPs), 5.2% long-chain chlorinated olefins (LCCOs), 15.2% long-chain chlorinated diolefins (LCCdiOs) and 56.4% long-chain chlorinated triolefins (LCCtriOs) were found (Tables S4–S7). Moreover, when the minor C- and Cl-homologues of sample P4 are zoomed in, a second maximum is observed for CdiOs at C_{17}- and CtriOs at C_{19}-homologues. This was not found in P1, P2 nor P3, which highlights the variability of the C- and Cl-homologue distributions. GC-ECNI-MS data of samples P2 and P3, which were reported previously, were compared with LC-APCI-MS data (Schinkel et al., 2018a). The former data were evaluated by RASER for the first time and broader C-homologue distributions were detected. Only SCCP content was published, whereas C_{10}- to C_{17}- and C_{10}- to C_{16}-homologues could be found for P2 and P3, respectively (Figure S4 and Tables S8 and S9). Chlorination degrees from Cl_6 to Cl_{11} were reported for both P2 and P3 by the GC-ECNI-MS method. However, Cl_4- to Cl_{13}- and Cl_{11}- to Cl_{12}-homologues were found when P2 and P3 were analyzed by LC-APCI-MS, respectively. Both datasets showed similar unimodal distributions in terms of C- and Cl-homologues. However, Cl-homologue distributions are shifted substantially towards higher-chlorinated material, if the GC-ECNI-MS data are considered. This is discussed further on.

3.3. Pattern study of plastic consumer products

Characteristic patterns were deduced based on the different C- and Cl-homologue distributions of CPs, COs, CdiOs and CtriOs. These patterns are peculiar for the individual materials shown here, for example, for four plastic consumer goods. Therefore, fingerprinting of CPs and

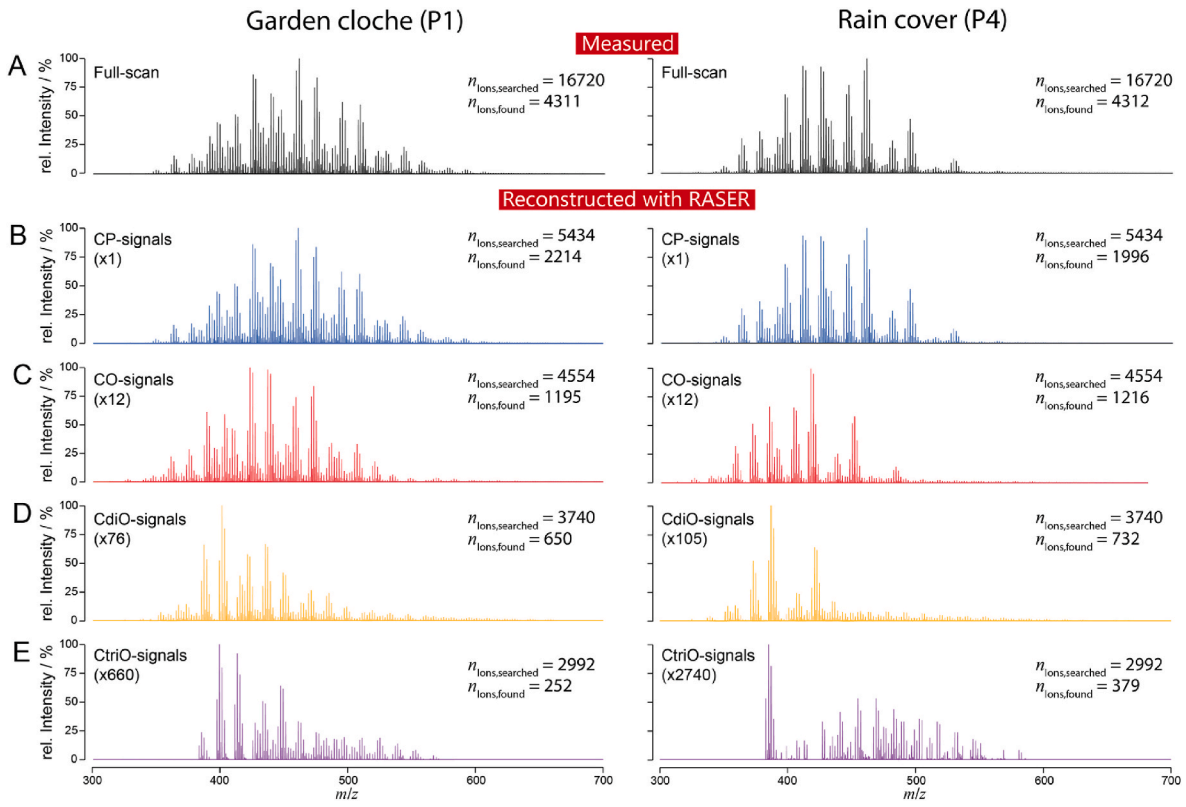

Fig. 1. Measured full-scan mass spectra (A) and reconstructed mass spectra (RMS) of CPs (B), COs (C), CdiOs (D) and CtriOs (E) of plastic consumer products P1 and P4. Samples were analyzed by LC-APCI-Orbitrap-MS. RMS were obtained from RASER. Number of ions searched for, the number of ions detected and zoom factors based on the most abundant homologues are depicted. Respective spectra of plastic material P2 and P3 (Figure S2) and data (Table S1) are given as supporting information.

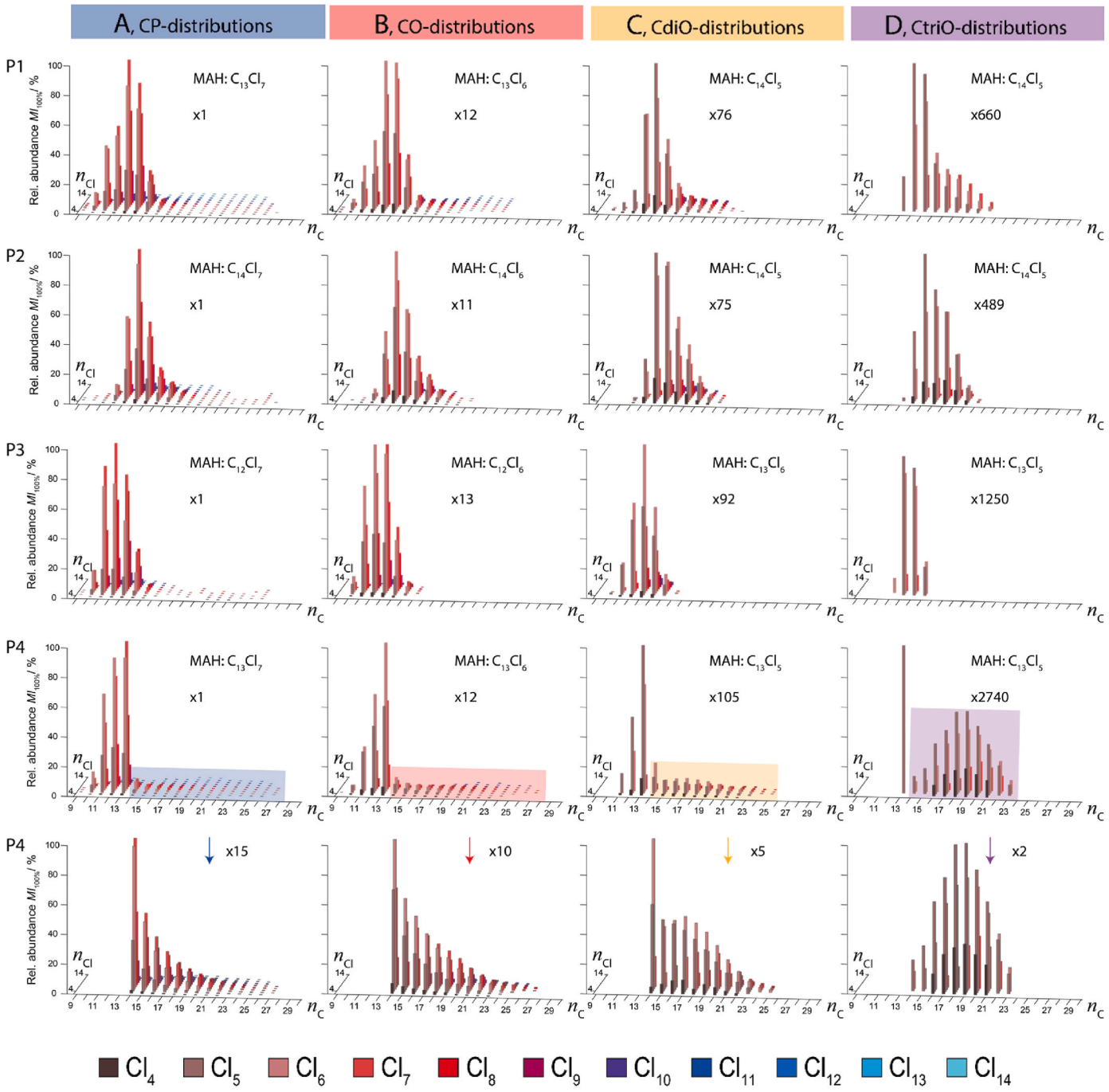

Fig. 2. Distribution of C-/Cl-homologues of CPs (A), COs (B), CdiOs (C) and CtriOs (D) in plastic consumer products P1–P4 analyzed by LC-APCI-Orbitrap-MS and RASER. Most abundant homologues (MAH, 100%) and zoom factors are indicated. In addition, zoomed diagrams of the MC-, LC- and vLC-homologues of sample P4 are plotted, highlighting a shift to a second maximum (C_{17}–C_{19}) for chlorinated di- and tri-olefins. Respective data are given as supporting information (Tables S4–S7).

their olefinic transformation products is an approach to compare samples of diverse origins. In the following chapters, we describe patterns based on different chain length classes (legal relevance) and saturation degrees. Furthermore, Cl-homologues distributions are produced for paraffinic and olefinic material. Additional patterns of mean carbon numbers (n_C) per Cl-homologue and mean chlorine numbers (n_{Cl}) per C-homologue are discussed.

3.3.1. Classification by chain length classes

The proportions (ρ) of very short-chain (vSC, C_9), short-chain (SC, $C_{10–13}$), medium-chain (MC, $C_{14–17}$), long-chain (LC, $C_{18–21}$) and very long-chain (vLC, $C_{\geq 22}$)-homologues of paraffinic and olefinic material of plastic items P1–P4 were calculated from the LC-APCI data (Fig. 3 and Table S10). The proportion of, e.g. SCCPs ($C_{10–13}$), can be calculated by the Equation (2).

$$\rho_{SCCPs} = \frac{\sum_{x=10}^{13}\sum_{y=4}^{14} MI_{100\%,C_xCl_y(CP)}}{\sum_{x=9}^{27}\sum_{y=4}^{14} MI_{100\%,C_xCl_y(CP)}} * 100 \quad \text{Eq. 2}$$

The proportions of short-chain material of P1 decrease from 59.8% for CPs to 49.9%, 26.4% and 3.6% for COs, CdiOs and CtriOs. On the

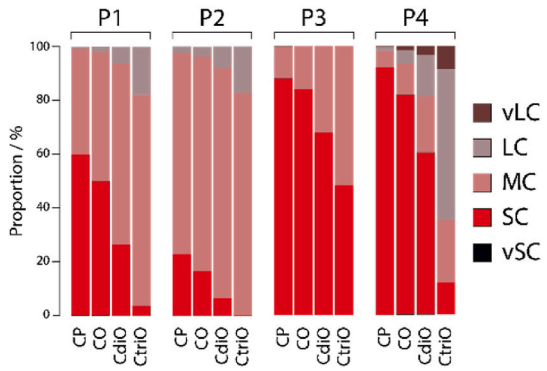

Fig. 3. Proportions of very short-chain (vSC, C_9), short-chain (SC, $C_{10\text{-}13}$), medium-chain (MC, $C_{14\text{-}17}$), long-chain (LC, $C_{18\text{-}21}$) and very long-chain (vL, $C_{\geq 22}$) homologue classes detected in CPs, COs, CdiOs and CtriOs in plastic consumer products P1–P4. Samples were analyzed by LC-APCI-Orbitrap-MS. SCCPs highlighted in red, which are regulated under the Stockholm Convention, are abundant in samples P1 (59.8%), P3 (88.2%) and P4 (92.2%) and less abundant in P2 (22.8%). Respective data are given as supporting information (Table S10). (For interpretation of the references to color in this figure legend, the reader is referred to the Web version of this article.)

other hand, proportions of medium-chain material increase from 39.2% for CPs to 47.9%, 67.3% and 78.4% for COs, CdiOs and CtriOs, respectively. Similar trends have been observed in the other samples. The high SCCP proportions of 88% and 92% in samples P3 and P4 and the proximity of these materials to humans are a concerning contamination source. CP patterns corresponding to carbon-chain length proportions were reported previously (Shen et al., 2023). However, the representation of the carbon-chain length proportion per saturation degree as a feature of the CP fingerprint was not reported before. Herein, we show that it can be used to discriminate between plastic materials of different origins. On the other hand, only CPs were reported in P2 and P3 by GC-ECNI-MS. The presence of olefinic material was not tested. SC- and MCCP contents were found in similar proportions for both samples by using GC-ECNI- and LC-APCI-MS (Figure S4).

3.3.2. Classification by saturation degree

The proportions (ρ) of CP-, CO-, CdiO- and CtriO-material were calculated for the items P1–P4 from the LC-APCI data (Fig. 4). The ratios between paraffinic and olefinic material of, e.g. C_9-homologues, in a plastic item can be calculated by the Equation (3).

$$\rho_{C_9(CP)} = \frac{\sum_{y=4}^{14} MI_{100\%,C_9Cl_y(CP)}}{\sum_{y=4}^{14} \left(MI_{100\%,C_9Cl_y(CP)} + MI_{100\%,C_9Cl_y(CO)} + MI_{100\%,C_9Cl_y(CdiO)} + MI_{100\%,C_9Cl_y(CtriO)}\right)} * 100 \quad \text{Eq. 3}$$

CPs were the most abundant compound class in every C-homologue (C_9 to C_{27}). The total olefinic signal (cts) accounted for 7.3%, 8.7%, 7.9% and 6.1% in the samples P1, P2, P3 and P4, respectively (Table S11). The proportions of olefinic material are not constant and increased with the carbon-chain length until maxima were reached and decreased again. Maxima of olefinic proportions were found for C_{20}- (21.2%), C_{19}- (15.2%), C_{15}- (13.1%) and C_{25}- (32.4%) homologues for P1, P2, P3 and P4 (Tables S12–S13). The increase of olefinic content with the carbon-chain length suggests a higher probability of HCl-losses from long-chain material. However, this hypothesis was not tested. The observed decrease of olefinic proportions towards LC- and vLCCPs might be due to low signal intensities. The results obtained for the sample P2 agree with the ones previously reported (Knobloch et al., 2022a). The loss of HCl induced by the ionization source was previously reported and this effect might change the pattern. However, the MS-settings remained the same for all samples. To discern whether olefinic material is formed during the CP production or processing of the plastic, further research is required. These results should rise awareness about the composition of such mixtures with relevant and characteristic proportions of olefinic material, which was overlooked until recently. Herein, we showed that olefinic material may count up to 30% for certain C-homologues. Olefinic compounds proved to be more persistent against transformation reactions catalyzed by the bacterial dehalogenase enzyme LinB (Knobloch et al., 2021). Therefore, the presence of olefinic material might affect the persistence, bioaccumulation potential and toxicity.

3.3.3. Classification by chlorine homologue distribution

The numbers and levels of chlorine homologues vary in technical CP mixtures depending on the supplier (Knobloch et al., 2022b). Due to that and the specific production conditions of plastic items, distinctive chlorine homologue distributions are expected. The proportion of a Cl-homologue of, e.g. C_9-homologues, can be calculated by using the Equation (4).

$$\rho_{C_9Cl_y(CP)} = \frac{MI_{100\%,C_9Cl_y(CP)}}{\sum_{y=4}^{14} MI_{100\%,C_9Cl_y(CP)}} * 100 \quad \text{Eq. 4}$$

In P1, P2, P3 and P4, $Cl_{4\text{–}14}$-, $Cl_{4\text{–}13}$-, $Cl_{4\text{–}12}$- and $Cl_{4\text{–}13}$-homologues were detected (Fig. 5 and S5 and Tables S14–S17). $Cl_{5\text{–}7}$-CPs were abundant in the vSC- and SC-homologues (C_9–C_{13}) of P1, accounting for ~90% of the counts. Higher-chlorinated homologues (Cl_{11}–Cl_{14}, blue) predominated throughout LCCPs (C_{20}, ~80%). Similar trends can be observed for P4. The chlorination degree increases in general with the carbon-chain length until a maximum is reached and decreased again. Samples P2 and P3 show an increase of the chlorination degree with the carbon-chain length too, but do show an abrupt increase of lower-chlorinated material at around C_{21} (Figure S5). This indicates that these plastic materials contain CPs of different origins. Due to LCCP material containing more hydrogen atoms than SC- and MCCPs, more hydrogens can be substituted by chlorines. This is reflected in Fig. 5 as an increase of the chlorine number with carbon-chain lengths, depicted in the plastic samples P1 and P4 as a gradual change of color from brown (Cl_4) to light blue (Cl_{14}). Generally, the olefinic material contained more lower-chlorinated homologues than the paraffinic ones. For example, $Cl_{4\text{–}13}$-, $Cl_{4\text{–}10}$- and $Cl_{4\text{–}7}$-homologues were found for COs, CdiOs and CtriOs in P1, respectively. Stepwise losses of HCl from parent CPs would result in lower chlorination degrees with decreasing saturation degree. Such processes agree with the observed CO-, CdiO- and CtriO-patterns. The pattern of sample P2 matches the one reported by Knobloch et al. However, the GC-ECNI-MS data showed a narrower range of Cl-homologues. $Cl_{6\text{–}12}$- and $Cl_{6\text{–}11}$-homologues were found in P2 and P3, while Cl_4–Cl_{13}-and Cl_4–Cl_{12}-homologues appeared in LC-APCI-MS data (Figure S6 and Tables S18–S19). The applied method could not detect Cl_4-and Cl_5-homologues and strongly suppressed Cl_6-homologues. However, the trends throughout the C-homologues are comparable in both methods.

3.3.4. Classification by carbon- and chlorine-number

Mean carbon- (n_C) and chlorine- (n_{Cl}) numbers can be calculated per chlorination degree and carbon-chain length respectively as shown in Equations (5) and (6) for, e.g. Cl_4- and C_9-homologues. Furthermore, weighted mean carbon and chlorine numbers can be calculated for each plastic sample including all C-/Cl-homologues by the Equations (7) and (8).

$$n_{C(Cl_4(CP))} = \sum_{x=9}^{27} \rho_{C_x Cl_4(CP)} {}^{*}x \quad \text{Eq. 5}$$

$$n_{Cl(C_9\ (CP))} = \sum_{y=4}^{14} \rho_{C_9 Cl_y(CP)} {}^{*}y \quad \text{Eq. 6}$$

$$n_{C\ (CP)} = \sum_{y=4}^{14} \sum_{x=9}^{27} \rho_{C_x Cl_y(CP)} {}^{*}x \quad \text{Eq. 7}$$

$$n_{Cl\ (CP)} = \sum_{x=9}^{27} \sum_{y=4}^{14} \rho_{C_x Cl_y(CP)} {}^{*}y \quad \text{Eq. 8}$$

where ρ_{CxCly} is the proportion of a C-/Cl-homologue, x is the number of carbons and y is the number of chlorines of a certain C- and Cl-homologue, respectively. Such numbers are characteristic for each plastic product and can be used as classification parameters (fingerprints). In all cases, the carbon numbers (n_C) per chlorination degree show minima at $Cl_{5–6}$ and an increase with the chlorination degree (Fig. 6 and S7 and Tables S20–S21). The variation throughout the Cl-homologues is more noticeable in P1 and P4 than in P2 and P3. Increasing n_C-numbers towards higher chlorinated homologues are observed for COs, CdiOs and CtriOs, too. The weighted mean carbon number (red line) in P1 increased from 13.1 for CPs to 13.5, 14.5 and 15.7 for COs, CdiOs and CtriOs, respectively. The n_C values published by Knobloch et al. are comparable to the ones reported herein, whereas the n_C values obtained by GC-ECNI slightly varied by 0.2 and 0.1 for the samples P2 and P3, respectively (Figure S6, Tables S20 and S21). Therefore, both analytical methods have similar sensitivities with respect to C-homologues.

Chlorine numbers (n_{Cl}) increase in all examples with the carbon-chain length until maxima are reached. Corresponding maxima were found for C_{21}-, C_{20}-, C_{16}- and C_{25}-CPs in P1, P2, P3 and P4, respectively (Fig. 6). A decrease of n_{Cl} towards LC- and vLCCPs was observed. This behavior was more pronounced for samples P1, P2 and P3 than in P4. Respective n_{Cl} trends were similar to the ones of COs, CdiOs and CtriOs but show systematic shifts towards lower n_{Cl} values. The weighted mean chlorine numbers (red line) in P1 decreased from 7.0 for CPs to 6.4, 5.9 and 5.8 for COs, CdiOs and CtriOs, respectively. Similar trends were observed in all samples. A steady decrease of the n_{Cl} was expected due to the stepwise HCl loss during the transformation of CPs to COs, CdiOs and CtriOs. The n_{Cl} values reported by Knobloch et al. for P2 match the ones reported herein. However, n_{Cl} values obtained from the GC-ECNI method were 1.5 and 1.1 higher than the ones from the LC-APCI method for P2 and P3, respectively. This is explained by the low sensitivity of the GC-ECNI-MS for Cl_4– Cl_5-and Cl_6-homologues.

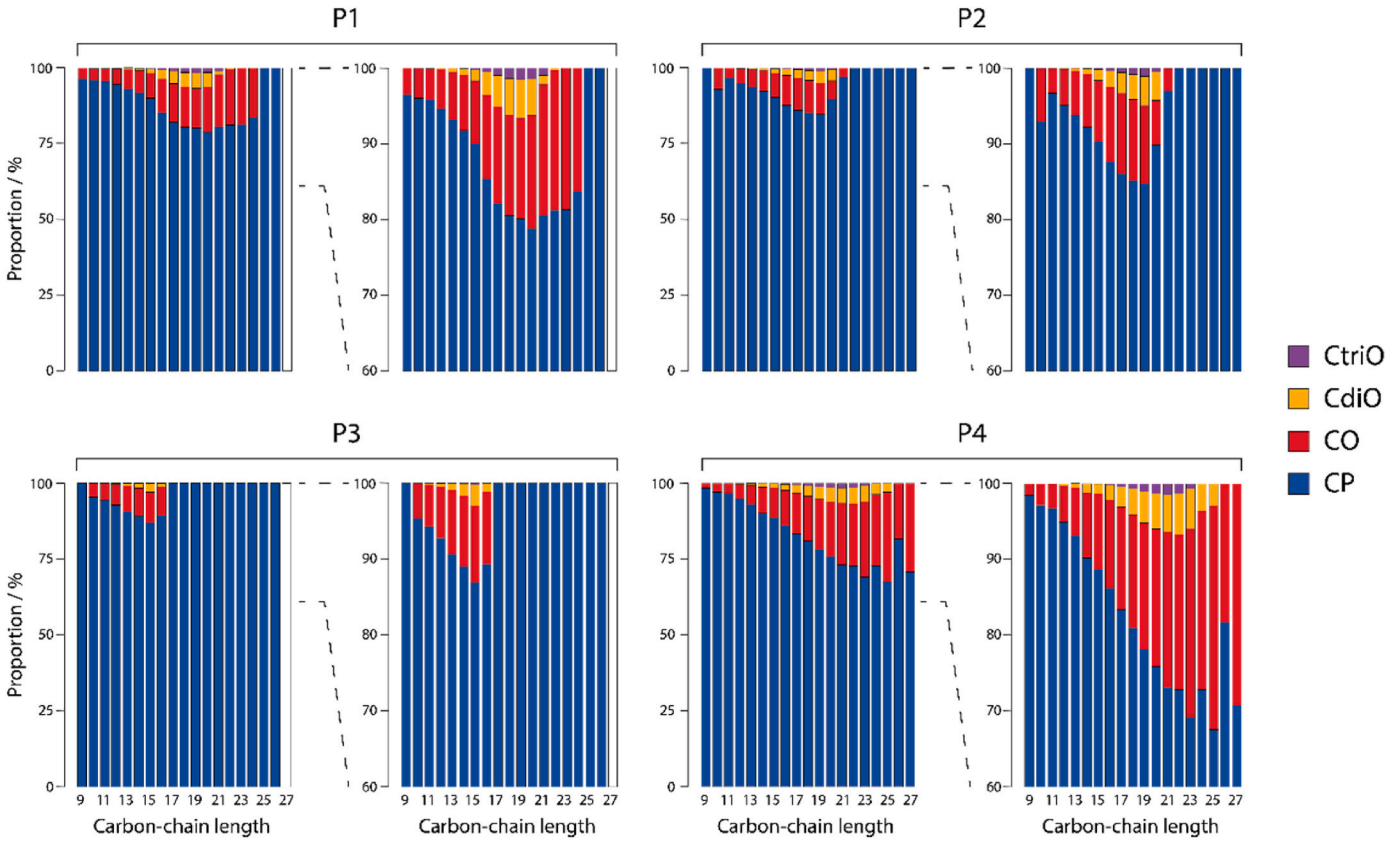

Fig. 4. Proportions of CPs (blue), COs (red), CdiOs (orange) and CtriOs (magenta) for different C-homologues ($C_{9–27}$) in plastic consumer products P1–P4. Samples were analyzed by LC-APCI-Orbitrap-MS and RASER. Respective data are given as supporting information (Tables S11–S13). (For interpretation of the references to color in this figure legend, the reader is referred to the Web version of this article.)

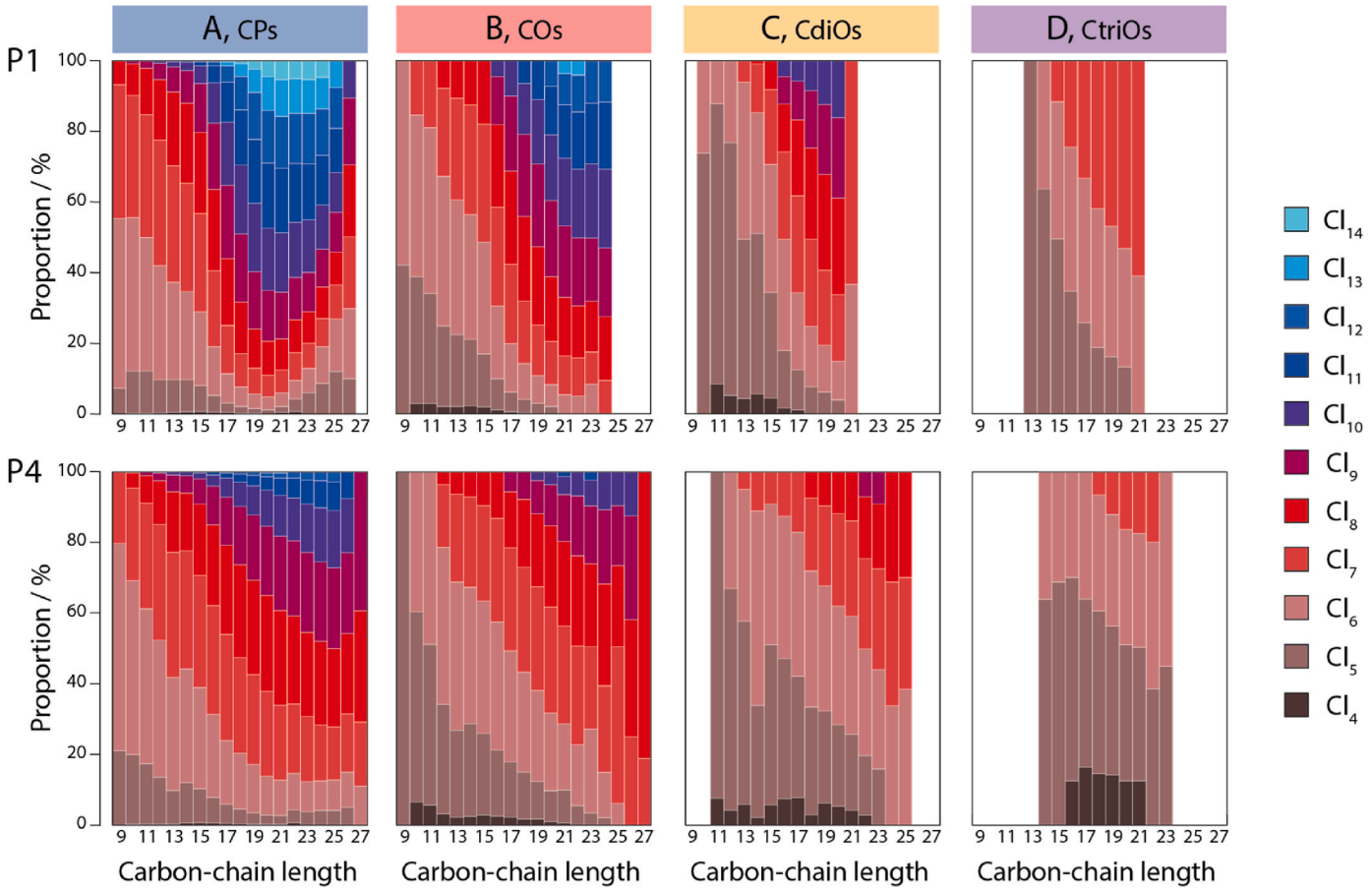

Fig. 5. Distributions of Cl-homologues per carbon-chain length of CPs (A), COs (B), CdiOs (C) and CtriOs (D) in plastic consumer products P1 and P4. Samples were analyzed by LC-APCI-Orbitrap-MS and RASER. Based on the given color code, different Cl-homologues can be distinguished. Respective figures of plastic material P2 and P3 (Figure S5) and data (Tables S14–S17) are given as supporting information. (For interpretation of the references to color in this figure legend, the reader is referred to the Web version of this article.)

4. Limitations of the method

CPs and their transformation products can be analyzed by diverse analytical techniques. However, different sensitivities towards both, C- and Cl-homologues, can provide mismatching fingerprints. According to the results reported here, the LC-APCI method was more versatile than the GC-ECNI one (Figure S4). Therefore, fingerprints obtained from two different analytical methods should be compared carefully (Figure S6). An Orbitrap mass analyzer is recommended to achieve the necessary mass spectral resolution (Figure S3). With it, MS signals corresponding to the adduct ions $[M+Cl]^-$ of CPs and their transformation products can be distinguished and further mathematical deconvolution methods can be avoided. Instrumental errors can cause pattern discrepancies. However, the fluctuations corresponding to the LC-APCI method for C- and Cl-homologues were below 10%. To ensure time-efficient data evaluation, large datasets should be assessed with an automatic data evaluation tool and fingerprint generator. Furthermore, reference materials should be chosen accordingly to match the targeted range of C- and Cl-homologue and matrices. Finally, the establishment of a library of fingerprints is critical for further research, such as the apportionment studies.

5. Conclusions

Fingerprints of CPs and their transformation products were obtained for four plastic consumer products from LC-APCI-Orbitrap-MS data. The proportion of carbon-chain length class per saturation degree was used for the first time to distinguish between plastic samples. In total, five parameters should be considered when fingerprints are obtained. The simplicity of the calculations allows rapid automation of the data evaluation to process large numbers of plastic samples and obtain a comprehensive library of materials. Such library can be used for future source apportionment studies to reduce environmental burdens and human exposure.

Fingerprints from GC-ECNI-Orbitrap-MS data could be obtained too. The comparison between GC-ECNI- and LC-APCI-MS data showed the versatility of the LC-method, which can detect a wider range of C- (up to C_{27}) and Cl-homologues (down to Cl_4). Pattern variabilities provided by both analytical techniques highlighted the different sensitivities towards C- and Cl-homologues. In other words, the fingerprinting method relies on the selected analytical technique. This should be considered when fingerprints obtained by different methods are compared. The combination of LC-APCI-Orbitrap-MS with RASER and the fingerprint method is a promising and efficient strategy to evaluate various plastic samples

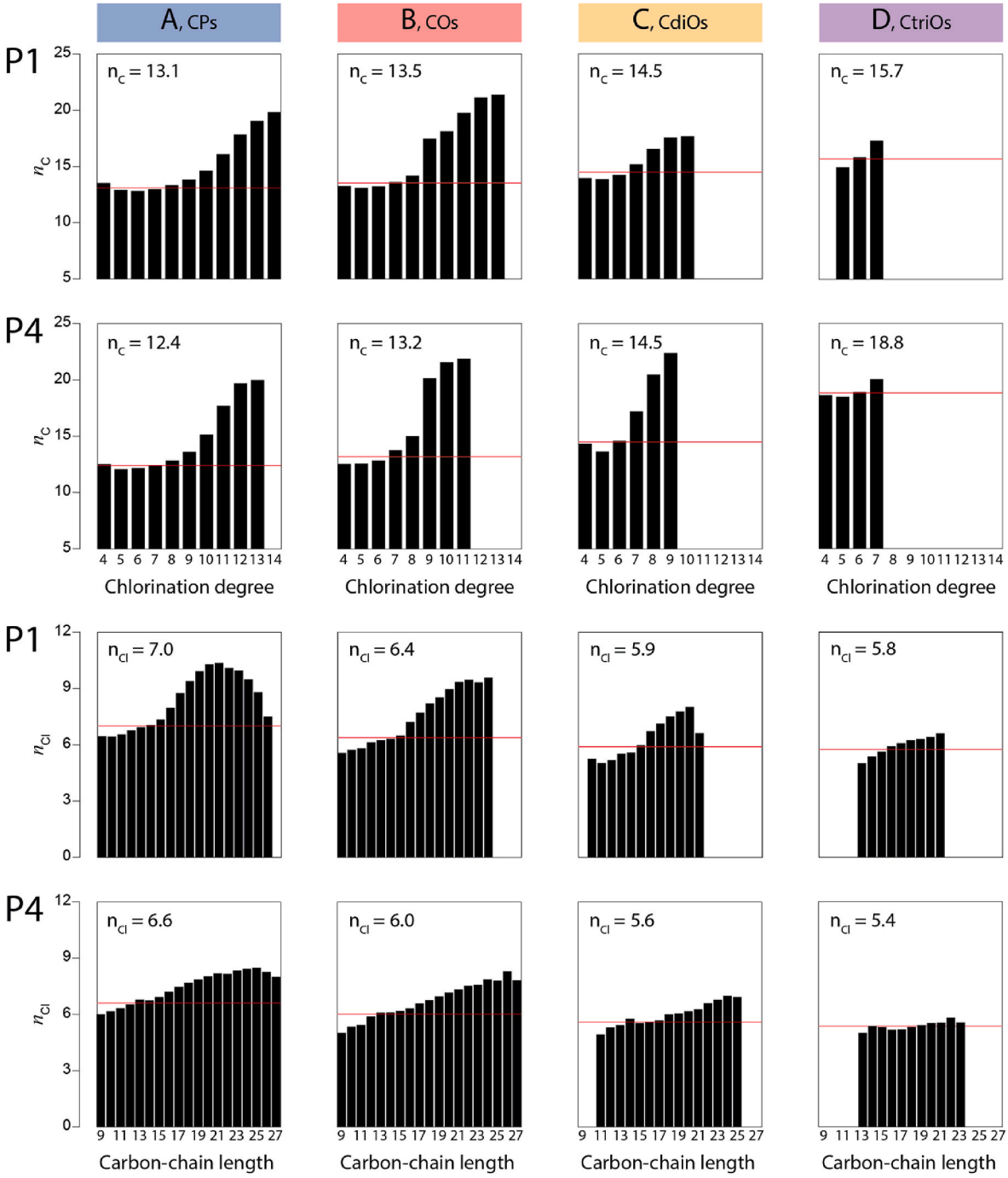

Fig. 6. Carbon- (n_C) and chlorine- (n_{Cl}) numbers of CPs (A), COs (B), CdiOs (C) and CtriOs (D). Carbon-numbers for different chlorination degrees (upper diagrams) and chlorine-numbers for different chain length (lower diagrams) are distinguished for P1 and P4. Samples were analyzed by LC-APCI-Orbitrap-MS and RASER. Weighted mean carbon and chlorine numbers are depicted (red lines). Respective figures of samples P2 and P3 (Figure S7) and data (Tables S20 and S21) are given as supporting information. (For interpretation of the references to color in this figure legend, the reader is referred to the Web version of this article.)

containing hundreds of C- and Cl-homologues. So far, this method was applied to four household items. However, we encourage to apply it on environmental and food samples. Fingerprints of CPs and other transformation products could be obtained as well. Furthermore, we recommend the use of several reference materials with similar matrices and C- and Cl-homologues as the target samples.

With this work, we also raise awareness of the disregarded content of olefinic material, which is produced, processed and released together with CPs. Therefore, such olefinic material should be subject of persistence, bioaccumulation and toxicity studies as well. Such studies may influence current and future CP regulations.

Credit authors statement

O. Mendo Diaz, Writing-Original Draft, Investigation, Writing-Review & Editing, Visualization, Formal analysis, Conceptualization, A. Tell, Investigation, Formal analysis, M. Knobloch, E. Canonica, Software, Methodologie, Writing-Review & Editing, Investigation, Formal analysis, C. Walder, Formal analysis, Writing-Review & Editing, A. M. Buser, Writing-Review & Editing, U. Stalder, Investigation, L. Bigler, Writing-Review & Editing, S. Kern, Writing-Review & Editing, D. Bleiner, Writing-Review & Editing, Supervision, N. V. Heen, Writing-Review & Editing, Supervision, Project administration, Funding acquisition, Conceptualization.

Declaration of competing interest

The authors declare that they have no known competing financial interests or personal relationships that could have appeared to influence the work reported in this paper.

Data availability

Data will be made available on request.

Acknowledgement

This work was supported by the Swiss Federal Office for the Environment (FOEN) (grant numbers: 00.5033.PZ/93F82B3A3 and 19.0011.PJ/CA22F4A93).

Four residual plastic samples studied in this work were provided by the Swedish Chemicals Agency (KEMI). Control sample used was provided by the Swiss Federal Office for the Environment (FOEN).

Supporting information

Supporting information is available free of charge on the Elsevier Publication website. It contains relevant figures of the data evaluation process, additional figures of samples P2 and P3, figures corresponding to the GC-ECNI-Orbitrap-MS analysis and tables with the corresponding data.

Appendix A. Supplementary data

Supplementary data to this article can be found online at https://doi.org/10.1016/j.chemosphere.2023.139552.

References

Barber, J.L., Sweetman, A.J., Thomas, G.O., Braekevelt, E., Stern, G.A., Jones, K.C., 2005. Spatial and temporal variability in air concentrations of short-chain (C-10-C-13) and medium-chain (C-14-C-17) chlorinated n-alkanes measured in the UK atmosphere. Environ. Sci. Technol. 39, 4407–4415. https://doi.org/10.1021/es047949w.

Brandsma, S.H., van Mourik, L., O'Brien, J.W., Eaglesham, G., Leonards, P.E.G., de Boer, J., Gallen, C., Mueller, J., Gaus, C., Bogdal, C., 2017. Medium-chain chlorinated paraffins (CPs) dominate in Australian sewage sludge. Environ. Sci. Technol. 51, 3364–3372. https://doi.org/10.1021/acs.est.6b05318.

Carney Almroth, B., Slunge, D., 2022. Circular economy could expose children to hazardous phthalates and chlorinated paraffins via old toys and childcare articles. J. Hazard. Mater. Adv. 7, 100107 https://doi.org/10.1016/j.hazadv.2022.100107.

Charbonnet, J.A., Rodowa, A.E., Joseph, N.T., Guelfo, J.L., Field, J.A., Jones, G.D., Higgins, C.P., Helbling, D.E., Houtz, E.F., 2021. Environmental source tracking of per- and polyfluoroalkyl substances within a forensic context: current and future techniques. Environ. Sci. Technol. 55, 7237–7245. https://doi.org/10.1021/acs.est.0c08506.

De Boer, J., 2010. Chlorinated Paraffins. Springer Berlin, Heidelberg, p. 2010. https://doi.org/10.1007/978-3-642-10761-0.

Fernandes, A.R., Vetter, W., Dirks, C., van Mourik, L., Cariou, R., Sprengel, J., Heeb, N., Lentjes, A., Krätschmer, K., 2022. Determination of chlorinated paraffins (CPs): analytical conundrums and the pressing need for reliable and relevant standards. Chemosphere 286, 131878. https://doi.org/10.1016/j.chemosphere.2021.131878.

Glüge, J., Wang, Z.Y., Bogdal, C., Scheringer, M., Hungerbühler, K., 2016. Global production, use, and emission volumes of short-chain chlorinated paraffins - a minimum scenario. Sci. Total Environ. 573, 1132–1146. https://doi.org/10.1016/j.scitotenv.2016.08.105.

Heeb, N.V., Schalles, S., Lehner, S., Schinkel, L., Schilling, I., Lienemann, P., Bogdal, C., Kohler, H.-P.E., 2019. Biotransformation of short-chain chlorinated paraffins (SCCPs) with LinA2: a HCH and HBCD converting bacterial dehydrohalogenase. Chemosphere 226, 744–754. https://doi.org/10.1016/j.chemosphere.2019.03.169.

Knobloch, M.C., Mathis, F., Diaz, O.M., Stalder, U., Bigler, L., Kern, S., Bleiner, D., Heeb, N.V., 2022a. Selective and fast analysis of chlorinated paraffins in the presence of chlorinated mono-, di-, and tri-olefins with the R-based automated spectra evaluation routine (RASER). Anal. Chem. 94, 13777–13784. https://doi.org/10.1021/acs.analchem.2c02240.

Knobloch, M.C., Schinkel, L., Kohler, H.-P.E., Mathis, F., Kern, S., Bleiner, D., Heeb, N.V., 2021. Transformation of short-chain chlorinated paraffins and olefins with the bacterial dehalogenase LinB from Sphingobium Indicum – kinetic models for the homologue-specific conversion of reactive and persistent material. Chemosphere 283, 131199. https://doi.org/10.1016/j.chemosphere.2021.131199.

Knobloch, M.C., Sprengel, J., Mathis, F., Haag, R., Kern, S., Bleiner, D., Vetter, W., Heeb, N.V., 2022b. Chemical synthesis and characterization of single-chain C18-chloroparaffin materials with defined degrees of chlorination. Chemosphere 291, 132938. https://doi.org/10.1016/j.chemosphere.2021.132938.

Krätschmer, K., Schächtele, A., Vetter, W., 2021. Short- and medium-chain chlorinated paraffin exposure in South Germany: a total diet, meal and market basket study. Environ. Pollut. 272, 116019 https://doi.org/10.1016/j.envpol.2020.116019.

Li, J., Xu, L., Zhou, Y., Yin, G., Wu, Y., Yuan, G.-L., Du, X., 2021. Short-chain chlorinated paraffins in soils indicate landfills as local sources in the Tibetan Plateau. Chemosphere 263, 128341. https://doi.org/10.1016/j.chemosphere.2020.128341.

Loos, M., Gerber, C., Corona, F., Hollender, J., Singer, H., 2015. Accelerated isotope fine structure calculation using pruned transition trees. Anal. Chem. 87, 5738–5744. https://doi.org/10.1021/acs.analchem.5b00941.

McGrath, T.J., Poma, G., Matsukami, H., Malarvannan, G., Kajiwara, N., Covaci, A., 2021. Short- and medium-chain chlorinated paraffins in polyvinylchloride and rubber consumer products and toys purchased on the Belgian market. Int. J. Environ. Res. Publ. Health 18. https://doi.org/10.3390/ijerph18031069.

Mézière, M., Cariou, R., Larvor, F., Bichon, E., Guitton, Y., Marchand, P., Dervilly, G., Le Bizec, B., 2020. Optimized characterization of short-, medium, and long-chain chlorinated paraffins in liquid chromatography-high resolution mass spectrometry. J. Chromatogr. A 1619, 460927. https://doi.org/10.1016/j.chroma.2020.460927.

Perkons, I., Pasecnaja, E., Zacs, D., 2019. The impact of baking on chlorinated paraffins: characterization of C10–C17 chlorinated paraffins in oven-baked pastry products and unprocessed pastry dough by HPLC–ESI–Q–TOF–MS. Food Chem. 298, 125100 https://doi.org/10.1016/j.foodchem.2019.125100.

Schinkel, L., Bogdal, C., Canonica, E., Cariou, R., Bleiner, D., McNeill, K., Heeb, N.V., 2018a. Analysis of medium-chain and long-chain chlorinated paraffins: the urgent need for more specific analytical standards. Environ. Sci. Technol. Lett. 5, 708–717. https://doi.org/10.1021/acs.estlett.8b00537.

Schinkel, L., Lehner, S., Heeb, N.V., Lienemann, P., McNeill, K., Bogdal, C., 2017. Deconvolution of mass spectral interferences of chlorinated alkanes and their thermal degradation products: chlorinated alkenes. Anal. Chem. 89, 5923–5931. https://doi.org/10.1021/acs.analchem.7b00331.

Schinkel, L., Lehner, S., Heeb, N.V., Marchand, P., Cariou, R., McNeill, K., Bogdal, C., 2018b. Dealing with strong mass interferences of chlorinated paraffins and their transformation products: an analytical guide. TrAC, Trends Anal. Chem. 106, 116–124. https://doi.org/10.1016/j.trac.2018.07.002.

Schinkel, L., Lehner, S., Knobloch, M., Lienemann, P., Bogdal, C., McNeill, K., Heeb, N.V., 2018c. Transformation of chlorinated paraffins to olefins during metal work and thermal exposure – deconvolution of mass spectra and kinetics. Chemosphere 194, 803–811. https://doi.org/10.1016/j.chemosphere.2017.11.168.

Shen, Y., Krätschmer, K., Bovee, T., Louisse, J., van Leeuwen, S.P.J., 2023. Chlorinated paraffins (CPs) in vegetable oils from the Dutch market and the effects of the refining process on their levels. Food Control, 109889. https://doi.org/10.1016/j.foodcont.2023.109889.

Tomasko, J., Stupak, M., Hajslova, J., Pulkrabova, J., 2021. Application of the GC-HRMS based method for monitoring of short- and medium-chain chlorinated paraffins in vegetable oils and fish. Food Chem. 355, 129640 https://doi.org/10.1016/j.foodchem.2021.129640.

UNEP, 2017. The United Nations Environment Programme-Decision SC-8/11: Listing of Short-Chain Chlorinated Paraffins. http://chm.pops.int/Portals/0/download.aspx?d=UNEP-POPS-POPRC.8-POPRC-8-11.English.pdf.

UNEP, 2021. The United Nations Environment Programme-Technical Work: Consideration of Chemicals Proposed for Listing in Annexes A, B And/or C to the

Convention: Chlorinated Paraffins with Carbon Chain Lengths in the Range C14-17 and Chlorination Levels at or Exceeding 45 Per Cent Chlorine by Weight, p. 339. UNEP/POPS/POPRC.17/6. https://wedocs.unep.org/bitstream/handle/20.500.11822/37141/21ig25_27_2519_eng.pdf.

Vorkamp, K., Balmer, J., Hung, H., Letcher, R.J., Rigét, F.F., 2019. A review of chlorinated paraffin contamination in Arctic ecosystems. Emerg. Contam. 5, 219–231. https://doi.org/10.1016/j.emcon.2019.06.001.

Wu, Y., Gao, S., Liu, Z., Zhao, J., Ji, B., Zeng, X., Yu, Z., 2019. The quantification of chlorinated paraffins in environmental samples by ultra-high-performance liquid chromatography coupled with Orbitrap Fusion Tribrid mass spectrometry. J. Chromatogr. A 1593, 102–109. https://doi.org/10.1016/j.chroma.2019.01.077.

Wu, Y., Ji, B., Zeng, X., Liang, Y., Gao, S., Yu, Z., 2022. Determination of long chain chlorinated paraffins in soils and sediments by high-performance liquid chromatography (HPLC) high resolution mass spectrometry (HR-MS). Anal. Lett. 55, 2590–2603. https://doi.org/10.1080/00032719.2022.2065678.

Yuan, B., Alsberg, T., Bogdal, C., MacLeod, M., Berger, U., Gao, W., Wang, Y., de Wit, C. A., 2016. Deconvolution of soft ionization mass spectra of chlorinated paraffins to resolve congener groups. Anal. Chem. 88, 8980–8988. https://doi.org/10.1021/acs.analchem.6b01172.

Yuan, B., Benskin, J.P., Chen, C.-E.L., Bergman, Å., 2018. Determination of chlorinated paraffins by bromide-anion attachment atmospheric-pressure chemical ionization mass spectrometry. Environ. Sci. Technol. Lett. 5, 348–353. https://doi.org/10.1021/acs.estlett.8b00216.

Yuan, B., Vorkamp, K., Roos, A.M., Faxneld, S., Sonne, C., Garbus, S.E., Lind, Y., Eulaers, I., Hellström, P., Dietz, R., Persson, S., Bossi, R., de Wit, C.A., 2019. Accumulation of short-, medium-, and long-chain chlorinated paraffins in marine and terrestrial animals from Scandinavia. Environ. Sci. Technol. 53, 3526–3537. https://doi.org/10.1021/acs.est.8b06518.

Zencak, Z., Oehme, M., 2004. Chloride-enhanced atmospheric pressure chemical ionization mass spectrometry of polychlorinated n-alkanes. Rapid Commun. Mass Spectrom. 18, 2235–2240. https://doi.org/10.1002/rcm.1614.

Zeng, L., Wang, T., Ruan, T., Liu, Q., Wang, Y., Jiang, G., 2012. Levels and distribution patterns of short chain chlorinated paraffins in sewage sludge of wastewater treatment plants in China. Environ. Pollut. 160, 88–94. https://doi.org/10.1016/j.envpol.2011.09.004.